Polysilicon thermal microactuators for heat scavenging and power conversion

Jorge Varona
Centro de Investigación en Ingeniería y Ciencias Aplicadas
Universidad Autónoma del Estado de Morelos
Avenida Universidad 1001
Cuernavaca, Morelos, Mexico 62209
and
McGill University
Department of Electrical and Computer Engineering
3480 University Street
Montreal, Quebec, Canada H3A-2A7
E-mail: varonae@ieee.org

Margarita Tecpoyotl-Torres
Centro de Investigación en Ingeniería y Ciencias Aplicadas
Universidad Autónoma del Estado de Morelos
Avenida Universidad 1001
Cuernavaca, Morelos, Mexico 62209

Anas A. Hamoui
McGill University
Department of Electrical and Computer Engineering
3480 University Street
Montreal, Quebec, Canada H3A-2A7

Jesús Ecobedo-Alatorre
Centro de Investigación en Ingeniería y Ciencias Aplicadas
Universidad Autónoma del Estado de Morelos
Avenida Universidad 1001
Cuernavaca, Morelos, Mexico 62209

Javier Sanchez-Mondragón
National Institute for Astrophysics, Optics and Electronics
Luis Enrique Erro No. 1
Tonantzintla, Puebla, Mexico 72000

Abstract. We describe the design and experimental characterization of two optimized thermal actuators devised to operate by means of scavenging heat from the environment. Different from the traditional MEMS thermal actuator that relies on electric current to generate heat by Joule effect, the devices presented here are optimized to absorb external heat and convert it into mechanical displacement and force. The behavior of vertical and horizontal microactuators fabricated in a standard surface micromachining process (PolyMUMPs, Research Triangle Park, North Carolina) demonstrates the viability of exploiting heat from the surrounding medium to realize batteryless microsystems. Analytical and finite element models are provided in support of the design. Results show that fairly large and useful displacements can be achieved at commonly available operating temperatures. *© 2009 Society of Photo-Optical Instrumentation Engineers.* [DOI: 10.1117/1.3152001]

Subject terms: microelectromechnical systems; actuators; thermal analysis; energy harvesting; modeling.

Paper 09004PR received Jan. 14, 2009; revised manuscript received Mar. 31, 2009; accepted for publication Apr. 22, 2009; published online Jun. 5, 2009.

1 Introduction

Microelectromechanical systems (MEMS) technology represents a paradigm in integration of complex engineering systems comprising control and data processing functions with sensing and actuation capabilities. Microactuator technologies find applications in a great variety of fields where a reduction in size and weight is important. Particularly compelling is the possibility of implementing MEMS and electronic circuitry together on the same substrate that can be manufactured in high volumes and low cost due to the mass production nature of semiconductor wafers.

However, the biggest technological barrier that prevents MEMS from reaching its full potential is the lack of an equally small power supply that can be included within the microsystem itself. Most MEMS devices require orders of magnitude more power than what is currently available from existing micropower sources. It is the need for an external bulky battery that hampers the feasibility and practicability of portable and wireless MEMS equipment.

The most viable power supply strategy for realizing autonomous MEMS (those unattached to an external power supply unit) is the one comprising energy harvesting from

1932-5150/2009/$25.00 © 2009 SPIE

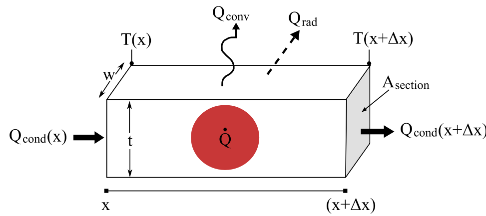

Fig. 1 Illustration of heat transfer by conduction, convection, and radiation in a solid differential element of length Δx.

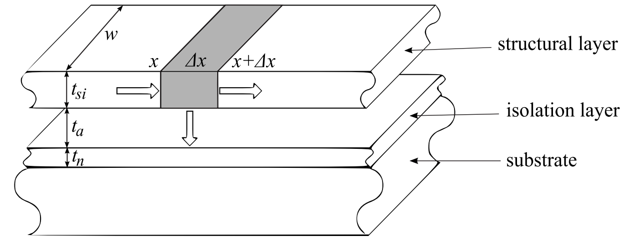

Fig. 2 Cross-sectional view of one section of a typical micromachined MEMS structure.

the environment and on-board energy storage elements. Accordingly, this work investigates a simplified power concept that does not involve the use of batteries nor dedicated wiring and control circuitry. Different from the classical electrically driven thermal actuator, this approach exploits heat from the environment to directly cause thermal expansion of the mechanical structures forming the actuator. Based on this idea, two different microactuators have been developed to offer vertical (out-of-plane) and horizontal (in-plane) actuation. Such conditions in which a high heat density is available are very common in practical situations where MEMS are usually found, for example in the automotive industry and in every application using electronic circuitry that dissipates heat.

Manufacturability and cost are critical parameters in determining the applicability of MEMS devices for industrial and commercial purposes. Thus, particular attention has been paid to preserve the mechanical simplicity of the actuators, minimizing the number of masks required for fabrication and avoiding the need for special materials and postprocessing microassembling steps.

2 Modeling and Design

2.1 *Thermal Distribution*

Three modes of heat transfer are involved in thermal modeling: conduction, convection, and radiation as depicted in Fig. 1. The heat losses by radiation may be ignored based on the fact that radiation becomes significant only at high temperatures ($>1000\,^\circ\mathrm{C}$),[1] while operating temperatures for polysilicon MEMS actuators are sufficiently low to neglect radiation effects.

The fundamental equation that describes the 3-D heat conduction problem is the so-called heat diffusion equation:

$$\nabla^2 T + \frac{\dot{q}}{k} = \frac{1}{\alpha}\frac{\partial T}{\partial t}, \tag{1}$$

where $\nabla^2 T = \partial^2 T/\partial x^2 + \partial^2 T/\partial y^2 + \partial^2 T/\partial z^2$ and $\alpha = k/\rho c$. T is the temperature distribution, α is known as the thermal diffusivity, k is the thermal conductivity of the material, ρ represents the density, c is the specific heat capacity, and $\dot{q}$ accounts for the possibility of volumetric heat generation within the element.

In the case of a thermally driven mechanical device, the most important issues of interest are the steady-state temperature increase, the temperature distribution along the microstructure, and the resulting net deflection of the actuator. Correspondingly, the partial differential heat diffusion in Eq. (1) can be fairly simplified by considering the static behavior under steady state and employing some reasonable assumptions. First, in a MEMS actuator that is fabricated using a surface micromachining process, the ratio of its length to crosssectional dimension is large, and the analysis can be treated as a 1-D problem. Secondly, as the device is intended to be externally heated, there is no volume heat generation within the element and Eq. (1) reduces to an ordinary differential equation in the form of:

$$\frac{d^2 T}{dx^2} = 0. \tag{2}$$

The 1-D heat transfer by conduction is given by Fourier's law according to Eq. (1):

$$Q_{\mathrm{cond}} = -kA_{\mathrm{section}}\frac{dT}{dx}, \tag{3}$$

where Q_{cond} is the conductive heat transfer rate in watts, k is the thermal conductivity of the material, A_{section} is the crosssectional area in the direction of heat flow, T is the temperature, and x is the 1-D axis in the direction of heat flow.

Convection accounts for the effect of heat transfer to the ambient through a fluid and can be described using Newton's law of cooling in Eq. (3):

$$Q_{\mathrm{conv}} = -hA_{\mathrm{surface}}(T_{\mathrm{element}} - T_a), \tag{4}$$

where h is the convection coefficient, A_{surface} is the surface area that experiments convective heat transfer to the air, T_{element} is the temperature in the surface of the object under analysis, and T_a is assumed to be the ambient temperature.

Figure 2 presents the crosssection view of a typical polysilicon structure in a surface micromachining technology[2,3] showing the different layers and materials employed for its fabrication. The first layer of silicon nitride (Si_3N_4) provides electrical isolation from the silicon substrate of the chip; a layer of polycrystalline silicon (polySi) is used as the structural layer for the microactuator. The size of the air gap between the polysilicon and the nitride layers is typically 2 μm but depends on the actual level of the polysilicon layer chosen by the designer.

Following the first law of thermodynamics for steady-state conservation of energy, and substituting $A_{\mathrm{section}} = w^* t_{si}$ and $A_{\mathrm{surface}} = w^* \Delta x$, the energy conducting into the element at point x is equal to the energy conducting out at point $x+\Delta x$ plus the energy which is transferred by convection to the ambient:

Table 1 Material properties.

Material properties	Value	Units
Density ρ	2.2×10^{-15}	kg/μm^3
Specific heat capacity c	$1\times10^{+2}$	J/Kg K
Thermal expansion α	4.7×10^{-6}	C^{-1}
Thermal conductivity of polysilicon k_p	148×10^{-6}	W μm^{-1} C^{-1}
Convection coefficient h	10×10^{-12}	W/μm^2 K

$$-kwt\left.\frac{dT}{dx}\right|_{x}=-kwt\left.\frac{dT}{dx}\right|_{x+\Delta x}+hw(T-T_a)\Delta x, \tag{5}$$

where T is the operating temperature, and the material properties are assumed to be uniform throughout the structure's length with respect to temperature. After rearranging Eq. (5) and taking the limit as $\Delta x\to0$, the following second-order differential equation is obtained:

$$\frac{d^2T}{dx^2}-\frac{h}{kt}(T-T_a)=0. \tag{6}$$

Equation (6) is nothing but the steady-state 1-D heat diffusion equation presented in Eq. (2) minus the term allowing for the convection effect. If changing variables in the form of $\theta=T-T_a$ and $B=\sqrt{h/kt}$, the general solution for Eq. (6) is:

$$T_{(x)}=T_s+C_1\exp(Bx)+C_2\exp(-Bx). \tag{7}$$

A particular solution for boundary conditions $\theta_{(0)}=\theta_2$ and $\theta_{(L)}=0$ yields:

$$C_1=\frac{\theta_2}{1-\exp(2BL)},\quad C_2=\theta_2-C_1. \tag{8}$$

The material properties used for analysis and simulations are listed in Table 1. Estimation of the heat convection coefficient is a nontrivial task, as it can change dramatically from one situation to the next. It also depends on the operating environment of the actuator, on the location of the external heat source, and its interaction with the device, whether the heat is applied through the substrate to the anchor pads or to one of the pads exclusively, if the device has been released from the original substrate, etc.

2.2 *Thermal Expansion and Deflection*

Once the temperature distribution is available, a model for the thermal expansion can be developed using the following set of linear equations:

$$\Delta L=K^{-1}F_{\text{thermal}},\quad F_{\text{thermal}}=A\sigma,\quad \sigma=E\alpha\Delta T, \tag{9}$$

where K is the stiffness coefficient, A is the cross sectional area, E corresponds to Young's modulus $\Delta T=(T-T_a)$, σ represents the thermal stress, and α is the thermal expansion coefficient of the material.

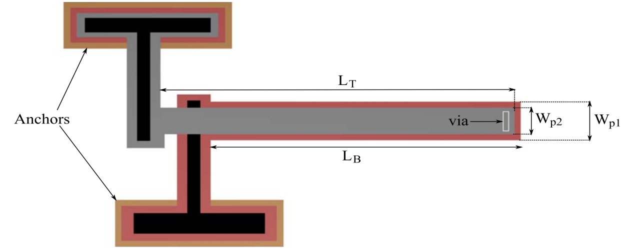

Fig. 3 Schematic drawing of the optimized double-beam vertical thermal actuator.

The thermal expansion for the polysilicon structure is obtained by integrating along its length:

$$\Delta L=\alpha\int_0^L(T-T_a)dx, \tag{10}$$

substituting the appropriate temperature distribution from Eq. (7) gives:

$$\Delta L=\alpha\int_0^L[C_1\exp(Bx)+C_2\exp(-Bx)]dx. \tag{11}$$

Finally, the mechanical deflection of the actuators can be estimated based on the thermal expansion by using some of the well established structural engineering methods presented in previous works[4,5] that analyze the bending moments acting on the heated structures by solving a set of simultaneous equations.

2.3 *Design of Vertical Actuator*

Vertical actuators are useful for many applications requiring out-of-plane displacements. The basis for the operation of these devices consists in obtaining asymmetrical thermal expansion between two levels of adjacent and physically joined structural microbeams.

Variations of the vertical actuator are well documented.[5,6] One of the preferred architectures for implementing a vertical thermal actuator (VTA) comprises two U-shape structures, one on top of the other, that are connected at one end, which constitutes the tip of the actuator. If a voltage is applied between the anchor pads of the top level structure, electrical current will flow solely through this layer, thereby increasing its temperature and causing a correspondent thermal expansion that will deflect the tip of the actuator downward to the substrate. Similarly, if the voltage is established across the anchors of the lower level structure, a deflecting force will actuate upward away from the substrate.

This work reports a customized actuator design that generates vertical deflection as a result of external heating of the device. Because the heat is not generated internally by Joule effect, the U-shape or other closed-loop topologies previously proposed for the design of vertical thermal actuators are not required, since no electrical circuit needs to

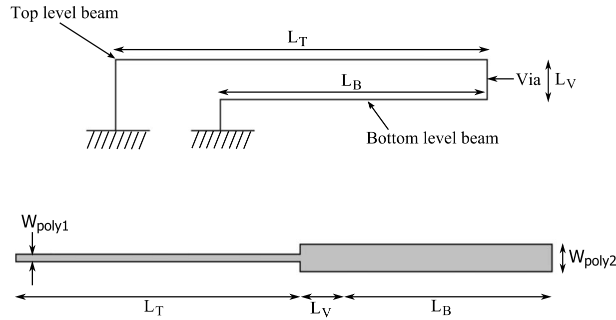

Fig. 4 Simplified coordinate system and schematic diagram of the unfolded actuator of Fig. 3, showing the two microbeams connected in a series.

be formed. A simplified geometry that does not entail providing a return path to ground for a driving current is introduced in Fig. 3.

The structure is formed by two cantilever-type beams fabricated in two different layers one on top of the other and separated by an air gap. The beams are independently anchored on the substrate at one end and linked to each other at the other end by means of a via. The width of the upper cantilever is made smaller than that in the lower level so that the beams are asymmetric. Also, the top layer is about 25% thinner than the bottom one due to characteristics imposed by the target fabrication process.

In the presence of a heat source, energy is transferred to the structure of the actuator, which in turns increases its temperature. The different geometry of the two microbeams leads to a net expansion of the top layer structure that generates vertical deflection in the direction of the substrate. Bidirectional displacement can be achieved if heat is applied separately through one of the anchors. In such a case, the temperature along the actuator will decrease as one moves in the direction of heat flow, as dictated by heat transfer theory. Accordingly, one of the beams will expand more than the other, driving the tip of the actuator against the colder beam.

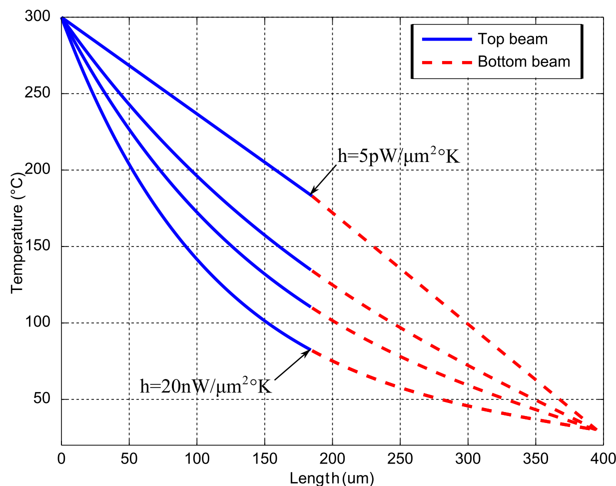

Fig. 5 Solution for temperature distribution along the actuator beams for different values of the convection coefficient *h*.

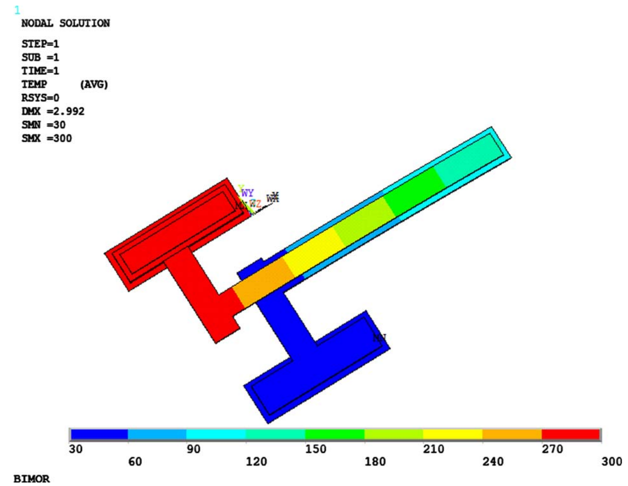

Fig. 6 Numerical results from FEM simulations for the temperature distribution of the vertical actuator.

The design concept relies on the availability of a sufficiently high heat source. External heat sources are fairly common in environments where MEMS find practical use. Examples include the automotive and aerospace industry, where high heat transfer rates and temperatures beyond 500 °C are commonly available.[7] Another potential widespread source of heat for MEMS is found in modern electronic very large scale integration (VLSI) integrated circuits that may have power densities in excess of 40 W/cm^2.[8,9]

The thermal analysis of the vertical thermal actuator depicted in Fig. 3 treats the two microbeams as elements that are connected in a series, as depicted in the schematic of Fig. 4. The total length of the device is $L_T+L_V+L_B$, with the segment L_B being thicker than L_T as indicated before. The following analysis also assumes that heat is applied at the anchor pad of the upper beam, while the anchor of the lower beam is kept in contact with the substrate at room temperature.

The steady-state spatial thermal distribution can be derived based on Eqs. (7) and (8). Figure 5 presents an example for the thermal distribution along the beams of the vertical actuator with a total length of 395 μm. The effect of the exact value of the convection coefficient *h* on the

Table 2 Optimized dimensions of the vertical thermal actuator.

Geometrical parameter	Value	Units
Length of top beam	185	μm
Length of bottom beam	210	μm
Width of top beam	18	μm
Width of bottom beam	26	μm
Thickness of top beam	1.5	μm

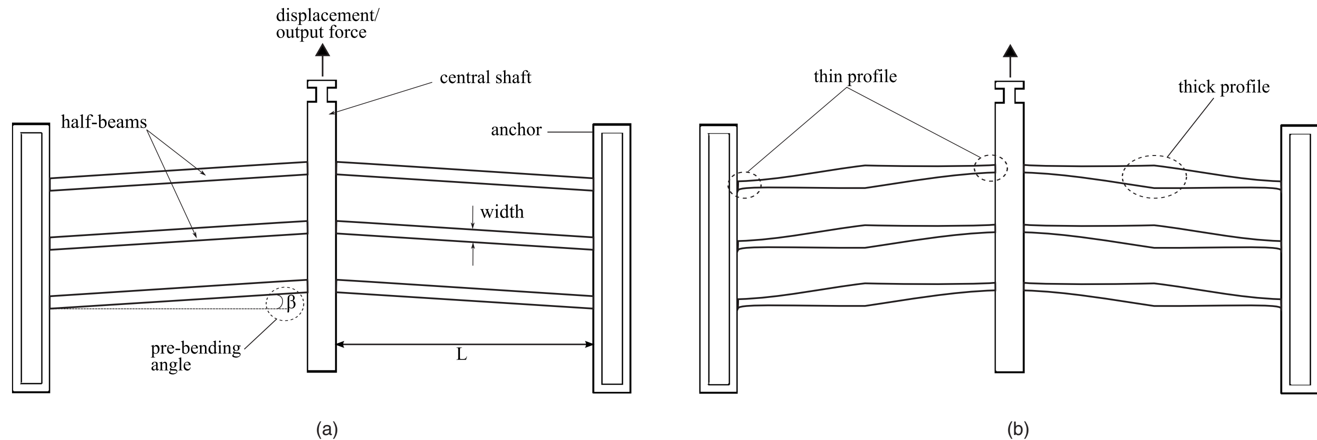

Fig. 7 Schematic drawing of the chevron or buckle-beam horizontal thermal actuator: (a) classical topology and (b) modified design.

temperature profile can be observed as the distribution changes from a linear to exponential shape. The final geometry of the actuator is given in Table 2.

The analytical results were verified using finite element models (FEMs) in computer simulations. In modeling, material properties and characteristic parameters of the optimized actuator were utilized as given in Table 1 and 2.

Figure 6 shows the temperature distribution of the thermal actuator when the anchor pad of the upper level microbeam is brought to 300 °C. Simulation results for the out-of-plane tip deflection of the actuator as a function of temperature behave as predicted by the analytic model in Ref. 10.

2.4 *Design of Horizontal Actuator*

For generating in-plane actuation, the chevron topology shown in Fig. 7(a) was chosen. The chevron actuator consists of an array of buckle-beam actuators fixed by anchors at both sides. When heated, the symmetrical thermal expansion of the opposing beams will cause them to buckle. The deflection of the chevron depends on a prebending angle β, and the length of the half beams L.

This kind of actuator offers a high actuation force per unit area, as many beams can be arrayed with no coupling penalty. The actuating force is proportional to the cross section of the beams; as such, a thicker beam made of a stack of two polysilicon layers might offer a higher output force. However, with the aim of simplifying manufacturing requirements, reducing costs, and further facilitating compatibility and integration with VLSI circuit technology, it was decided to use a single released micromachined layer entailing the need for just one photolithographic mask.

Due to its symmetrical expansion principle, the chevron topology is very well suited for operating from an external heat source that may evenly affect the device. The analysis of the chevron actuators was also based on the thermal distribution and thermal expansion models developed in Eqs. (7)–(11), estimating the expansion of each one of the beams individually. Once the increase in length ΔL is obtained, the deflection of the actuator can be estimated by:[11]

$$\mathrm{def}_{\mathrm{chev}} = [L^2 + 2L(\Delta L) - L\cos^2(\beta)]^{1/2} - L\sin(\beta), \qquad (12)$$

where L is the length of a single beam, ΔL is the elongation of the beam due to thermal expansion, and β is the prebending angle.

To improve the thermomechanical performance of the classical chevron actuator, a novel optimized design was also developed, as shown in Fig. 7(b). In the optimized actuator, the width of the buckle beams is no longer uniform but the middle section is made wider than the two extremes. This modification improves flexibility and relaxes mechanical constraints at the joints of the beams with the fixed anchors and with the movable central shaft. Basically, stored elastic energy at the joints is reduced, allowing the use of less energy for the actuator to deform itself and leaving more energy to perform useful work.

The contouring of the beam's ends yields a reduction in lateral stiffness and, in the case of an electrically driven chevron, the widening of the middle section provides a more uniform spatial distribution of temperature, avoiding hot spots and the risk of thermal failure of the device that can tolerate higher operating currents.

Table 3 Summary of dimensions for the two different test horizontal thermal actuators.

Configuration	Length of beams (μm)	Number of beams	Angle β (degrees)	Minimum width (μm)	Maximum width (μm)
Classical	200	8	2.3	2.75	2.75
Modified	200	8	2.3	2.50	6.0

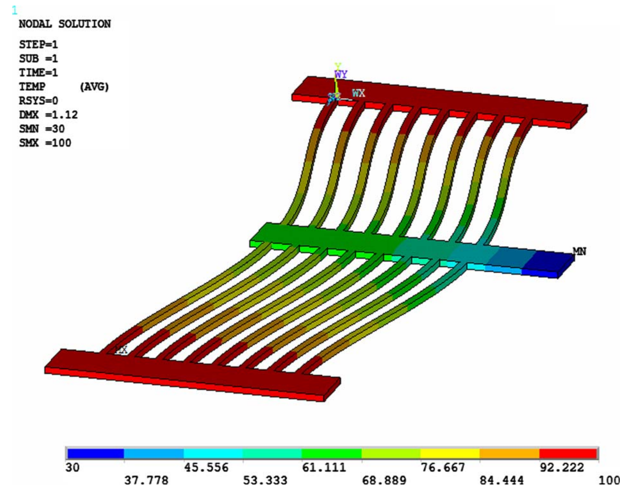

Fig. 8 Numerical simulation results for thermal distribution and deflection of a chevron actuator heated through its anchors.

The basic geometric parameters of the two fabricated chevron actuators are summarized in Table 3. The thermal distribution and thermal expansion along the beams of the modified actuator were calculated by breaking the beams into sections of different width and using a piecewise analysis approach based on Eqs. (7) and (10).

As in the design of the vertical actuator, finite element analysis (FEA) was also carried out to validate the design of the chevron actuators listed in Table 3. Multiphysics models including mechanical and thermal domains were used while imposing boundary conditions as mentioned before.

Figure 8 offers an example simulation result of displacement and thermal distribution along the surface of a chevron actuator when the heat source is applied from the substrate to its anchors.

3 Fabrication and Testing

The proposed thermal actuators were fabricated using the commercial Multi-User MEMS process (PolyMUMPs, MEMSCAP, Research Triangle Park, North Carolina) that can include three standard layers of surface micromachined polysilicon. The actuators were then released, removing the sacrificial PSG layer by a buffered hydrofluoric (HF) etchant. Scanning electron microscope (SEM) images of the fabricated actuators are shown in Figs. 9 and 10.

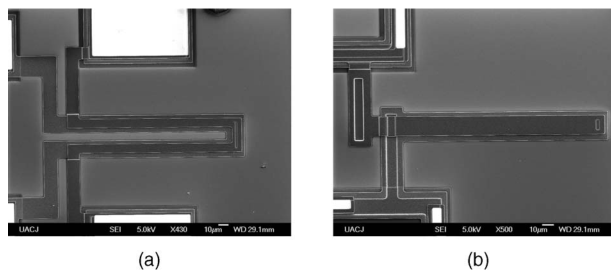

Fig. 9 SEM micrograph of the vertical actuators: (a) traditional U-shape actuator and (b) optimized double-beam actuator.

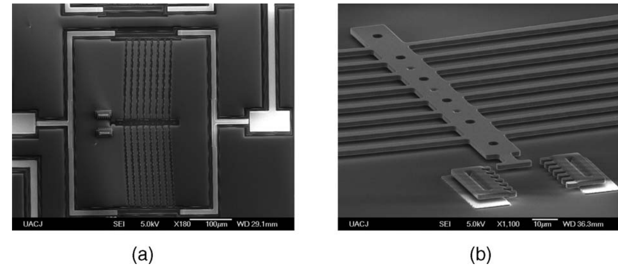

Fig. 10 SEM micrograph of the prototype modified chevron actuator: (a) top view and (b) 3-D view.

For characterization of the vertical thermal actuators, various test setups were used. The first one consisted in driving the actuators using traditional Joule heating by forming an electric circuit across the structure of the devices. In the second one, heat was selectively applied to a certain anchor pad(s) by mere solid thermal conduction. To do so, an electrical circuit was formed across the anchor pad alone without having any current flowing through the structure of the actuator; this setup permitted us to electrically control the temperature and the amount of energy applied at the anchor pad according to the Lenz-Joule law. A third experimental setup used an electric heating resistor to raise the temperature of the substrate of the whole microchip and actuate the devices by pure heat conduction.

Figure 11 presents a comparison between the performance of the U-shaped vertical actuator and the optimized double-beam configuration. It can be noticed that the U-shape VTA performs better than the double-beam configuration when the devices are actuated by the Joule effect. The reason for this is that the U-shape actuator provides an active return path for the current flow, where all the electrical power is used to heat only one layer of the device, while in the case of the double-beam VTA, the power consumed by the bottom layer has no contribution to the displacement of the actuator and is wasted in heating the lower beam that actually opposes the bending. However, when the actuators are driven by applying an external heat source, the double-beam VTA exhibits a better performance due to its simplified mechanical structure and lower convective surface that minimizes heat loss. It is worth mentioning that the maximum displacement in the direction of the substrate is limited by the height of the actuator from the substrate, which in this case is equal to 2 μm.

Figure 12 shows the experimental results for displacement of the horizontal chevron actuators as a function of pad temperature. The results demonstrate that the modified chevron actuator exhibits an improved mechanical performance compared to the traditional chevron with constant cross section beams.

The frequency response of the actuators was determined by alternately applying and ceasing to apply the heat source to one of the anchor pads. Experimentally, it was found that the vertical thermal actuators and the chevron actuators can operate at a frequency of up to 22 and 30 Hz, respectively, while still displaying full-swing deflection. Thermomechanical efficiency and frequency response strongly depend on how the heat is applied to the actuator and on the conditions for heat dissipation.

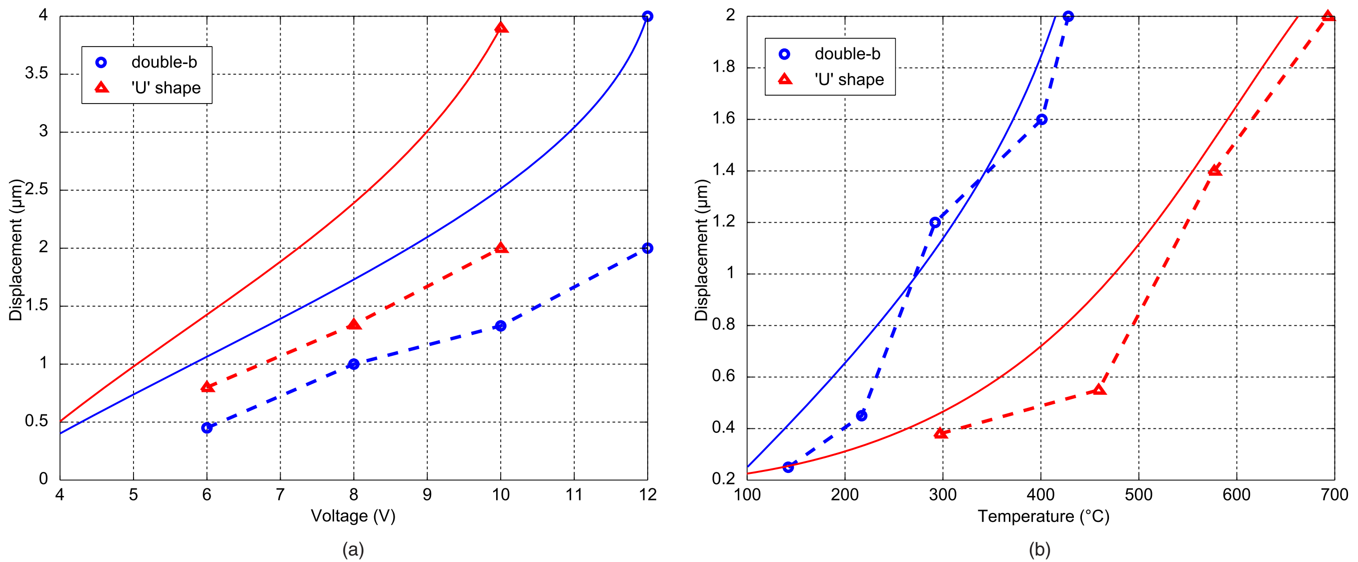

Fig. 11 A comparison of theoretical (solid lines) and experimental (dashed lines) results for the two VTA topologies. (a) Displacement as a function of voltage when actuated by the Joule effect. (b) Displacement as a function of temperature when actuated by external heating.

A comparison between measured and theoretical performance can been seen in Figs. 11 and 12. While there is good agreement between the analytical and experimental results for the displacement as a function of temperature, the discrepancies for the displacement versus voltage are significant. The cause of these differences is mainly due to variations between the estimated and actual temperature of the devices at a given input voltage. Conductive heat transfer through the anchor pads acting as heat sinks, and heat losses by convection through the surface of the structural beams, are the dominant heat dissipation mechanisms. Thus, when electrical heating is employed, the analytical model used for design and parameter optimization needs to be adjusted based on experimental data to account for the rate of thermal conduction to the anchor pads and to set the right value of the convection coefficient h.

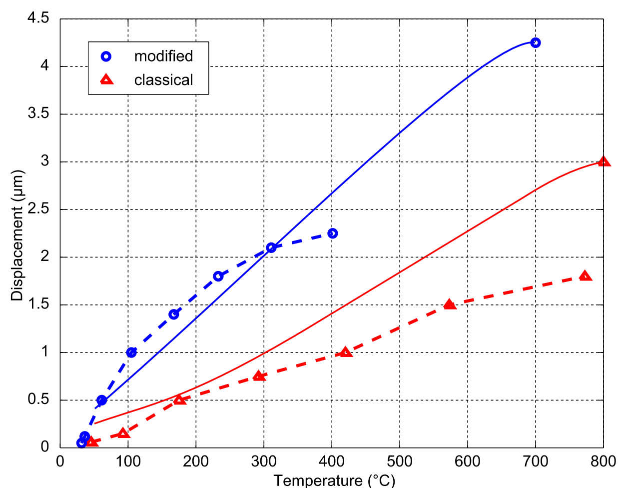

Fig. 12 Displacement as a function of the applied temperature for the two chevron actuator topologies under test. Solid lines represent the theoretical results.

4 Conclusions

The cofncept of leveraging the available heat in the environment to power autonomous MEMS devices appears extremely attractive. Potential applications for the externally heated VTA and chevron actuators include batteryless temperature sensors and thermal switches. Also, with the addition of a heat sink, a tunable thermal resonator can be implemented. Experimental results are encouraging, as relatively large displacements, useful for many practical applications, can be achieved by direct heating of the actuators. The enhanced performance of the optimized devices introduced in this work is an indication of the feasibility to implement these thermal actuators in many situations where an external heat source is already available. Among several prospective applications is the use of solar concentrators to heat arrays of thermal MEMS actuators driving a micropower generator within a chip. Potentially, any kind of heat source including solar radiation, lasers, hot air, conduction from a hot surface, etc., can be used to externally and wirelessly power the devices. Finally, the power consumption and efficiency issues of traditional thermal actuators are no longer of concern if the energy is taken from waste heat coming out of an engine, a VLSI circuit, etc.

Acknowledgments

The authors wish to thank Antonio Ramírez-Treviño from CINVESTAV-GDL, and José Mireles, Jr. and Perla García from UACJ for providing access to test equipment and laboratory facilities. Varona gratefully acknowledges financial support from a CONACYT scholarship and the Doctoral Scholars Loan from SAE.

References

1. R. Hickey, M. Kujath, and T. Hubbart, "Heat transfer analysis and optimization of two-beam microelectromechanical thermal actuators," *J. Vac. Sci. Technol. A* **20**(3), 971–974 (2002).
2. J. W. Gardner, V. K. Varadan, and O. O. Awadelkarim, *Microsensors MEMS and Smart Devices*, John Wiley and Sons, New York (2001).
3. J. Carter, A. Cowen, B. Hardy, R. Mahadevan, M. Stonefield, and S.

Wilcenski, *PolyMUMPS Design Handbook*, Revision 11.0, MEMSCAP Inc. (2005).
4. N. D. Mankame and G. K. Ananthasuresh, "Comprehensive thermal modeling and characterization of an electro-thermal-compliant microactuator," *J. Micromech. Microeng.* **11**, 452–62 (2001).
5. D. Yan, A. Khajepour, and R. Mansour, "Design and modeling of a MEMS bidirectional vertical thermal actuator," *J. Micromech. Microeng.* **14**, 841–850 (2004).
6. W. D. Cowan and V. M. Bright, "Vertical thermal actuators for micro-opto-electro-mechanical systems," *Proc. SPIE* **3226**, 137–146 (1997).
7. H. Fu, X. Chen, I. Shilling, and S. Richardson, "A one-dimensional model for heat transfer in engine exhaust systems," SAE Tech. Paper Series 2005-01-0696 (2005).
8. Y. Cheng, G. Xu, D. Zhu, W. Zhu, and L. Luo, "Thermal analysis for indirect liquid cooled multichip module using computational fluid dynamic simulation and response surface methodology," *IEEE Trans. Compon. Packag. Technol.* **29**(1), 39–46 (2006).
9. C. JM. Lasance and R. E. Simons, "Advances in high-performance cooling for electronics, electronics cooling," *Electron. Cool. Mag.* (2005), http://www.electronicscooling.com/articles/2005/2005_nov_article2.php.
10. Q. Huang and N. Lee, "Analysis and design of polysilicon thermal flexure actuator," *J. Micromech. Microeng.* **9**, 64–70 (1999).
11. M. J. Sinclair, "A high force low area MEMS thermal actuator," *Proc. Intersoc. Conf. Thermal Thermomechan. Phenom. Electron. Syst.*, 127–132 (2000).

Jorge Varona is a PhD candidate in the Research Center for Engineering and Applied Science at the State University of Morelos (UAEM). He received the MASc degree from the University of Toronto in 2002, and the BSc degree from Universidad Panamericana-Bonaterra in 1999. His professional experience and research interests are in the areas of VLSI integrated circuits and MEMS. He has been a design engineer for Tecno-Ingeniería Aplicada, Texas Instruments, and Snowbush Microelectronics. He is an associate researcher at Universidad Panamericana, and has been appointed as a member of the advisory board of the Mexican Microsystems Consortium (CMM).

Margarita Tecpoyotl-Torres received the BElectronics Eng. degree from the University of Puebla (BUAP), Mexico, in 1994, and the MSc and PhD degrees from the National Institute of Astrophysics, Optics and Electronics (INAOE), Mexico, in 1997 and 1999, respectively. In 1999, She joined the faculty at the Research Center for Engineering and Applied Sciences (CIICAp) of the State University of Morelos (UAEM), Mexico, where she is currently an associate professor and the academic coordinator of electrical engineering. Her current fields of interest are MEM and microwave devices.

Anas A. Hamoui received the BEng degree from Kuwait University in 1996, the MEng degree from McGill University in 1998, and the PhD degree from the University of Toronto in 2004, all in electrical engineering. Since 2004, he has been an assistant professor at the Department of Electrical and Computer Engineering, McGill University. His research emphasis is on analog-to-digital and digital-to-analog data converters. He is the coauthor (together with Ken Martin) of the book *Delta-Sigma Data Converters in Low-Voltage Nanometer CMOS for Broadband Digital Communication* (Springer, to be published in 2009). He was a recipient of the 2001 Outstanding Student Designer Award from Analog Devices Incorporated.

Jesús Ecobedo-Alatorre received the BSc degree in electrical engineering from the University of Guadalajara, Mexico, in 1994, and the MSc and PhD degrees from the National Institute of Astrophysics, Optics and Electronics (INAOE), Mexico, in 1997 and 2005, respectively. He is an assistant professor at the Research Center for Engineering and Applied Sciences (CIICAp) of the State University of Morelos (UAEM). His research focuses on communication systems and waveguides. He is also a member of the Mexican National System of Researchers (SNI-I).

Javier Sanchez-Mondragón received the bachelor's degree in physics from the National Autonomous University of Mexico (UNAM), and the PhD degree from the University of Rochester, New York, in 1980. He is a former president and cofounder of the Mexican Academy of Optics (AMO) that is affiliated to the Optical Society of America (OSA). He founded the quantum optics and lasers group at the Center for Research in Optics (CIO) in Mexico, and the photonics group at the National Institute of Astrophysics Optics and Electronics (INAOE), Mexico. He is a full professor at INAOE, a member of the Mexican National System of Researchers (SNI-III), and a fellow member of the Optical Society of America (OSA).